*Sedimentology* (1985) **32**, 133–145

# Experimental study of sand streaks formed in turbulent boundary layers

SUZANNE D. WEEDMAN *and* RUDY SLINGERLAND

*Department of Geosciences, The Pennsylvania State University, 507 Deike Building, University Park, PA 16802, U.S.A.*

## ABSTRACT

Fine- to medium-grained sand transported as bedload moves in lanes parallel to the flow that are thought to be preserved as parting lineation. A series of six flume experiments was designed to discover the morphology and spacing of these lanes, here called sand streaks, as functions of local shear velocity, $U_*$ ($9 \times 10^{-3}$ to $4{\cdot}8 \times 10^{-2}$ m s$^{-1}$), depth ($5 \times 10^{-2}$ and $9{\cdot}5 \times 10^{-2}$ m), mean grain diameter (150, 200, 290, 1380 μm), and sediment bedload concentration (0·0–0·39). Low $U_*$ flows produce predominantly straight, non-intersecting sand streaks, moderate $U_*$ flows produce sub-parallel and *en échelon* sand streaks, and moderate to high $U_*$ flows produce wavy sand streaks and secondary streaks with a spacing an order of magnitude larger. The wavy sand streaks are thought to be composed of sand grains in suspension close to the bed. An upper grain-size limit for the sand streak structure occurs at a grain size between 290 and 1380 μm. The spacings of the fine- and medium-grained sand streaks, at low to moderate $U_*$ ($0{\cdot}9 \times 10^{-2}$ to $3 \times 10^{-2}$m s$^{-1}$), are similar to those predicted for low-speed fluid streaks, although the fine-grained sand forms more closely-spaced streaks than the medium-grained sand. The spacings of sand streaks formed at moderate to high $U_*$ and at bedload concentrations greater than 0·15, are wider than those predicted for the low-speed fluid streaks. The wider spacing is thought to reflect a new type of flow immediately above the moving bed layer in which the formation of low-speed streaks is inhibited. This results from an increase in either grain concentration or grain size. The spacing of parting lineation, also wider than that predicted for low-speed streaks, may reflect this.

## INTRODUCTION

Fine- to medium-grained sand transported by turbulent flows as bedload moves in lanes parallel to flow, here called sand streaks. The sand streaks are a few grain diameters high, $3{\cdot}0 \times 10^{-2}$ to $2{\cdot}0 \times 10^{-1}$ m long, and transversely spaced from $2{\cdot}0 \times 10^{-3}$ to $2{\cdot}5 \times 10^{-2}$ m, thus producing a ridge and groove microtopography of intermittently moving grains (Sorby, 1908; Stokes, 1953; Allen, 1964; Karcz, 1970, 1973). The streaks are of interest because they offer insight into the nature of the flow and associated bedload transport in turbulent boundary layers. In addition, the ridges and grooves are hypothesized to be preserved as parting lineation in fine- to medium-grained sandstones (Allen, 1964, 1968, 1970, 1982; Karcz, 1970, 1973; Allen & Leeder, 1980; Leeder, 1981), and their spacing has been suggested as an indicator of flow intensity at the time of deposition (Allen, 1982).

Allen (1964) suggested that the structures could be explained best by the presence of streamwise, counter-rotating pairs of tubular vortices. These organized, quasi-periodic vortical structures now are well documented in turbulent boundary layers over smooth boundaries (review in Cantwell, 1982). The convergent and divergent zones result in alternating lanes of high- and low-speed fluid streaks that are formed and destroyed during the burst cycle (Kline *et al.*, 1967; Smith & Metzler, 1983). Several experimental methods using various fluids have confirmed a dimensionless spanwise spacing (Fig. 1) of the low-speed streaks to be :

$$\bar{\lambda}_z{}^+ \equiv \frac{\bar{\lambda}_z U_*}{\nu} \simeq 100 \pm 20 \qquad (1)$$

where $\bar{\lambda}_z$ is the arithmetic mean transverse spacing between streaks, $U_*$ is the shear velocity, and $\nu$ is the kinematic viscosity of the fluid (Bakewell & Lumley,

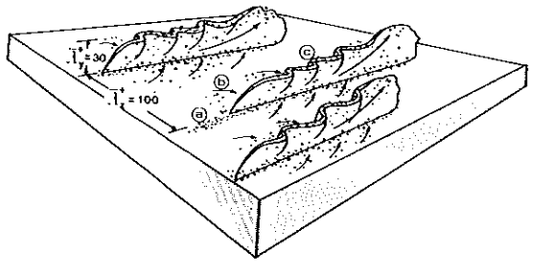


**Fig. 1.** Proposed model for the origin of sand streaks (A) within and (B) adjacent to lifting low-speed streaks. The dimensionless spanwise spacing of the low-speed streak is $\bar{\lambda}_z^+ \equiv \bar{\lambda}_z U_*/\nu \simeq 100 \pm 20$ and their dimensionless height is $\bar{\lambda}_y^+ \equiv \bar{\lambda}_y U_*/\nu \simeq 30$. Arrows on the bed indicate *en échelon* oblique flow paths of paired counter-rotating vortices formed from lifting and stretching the central portion of a spanwise vortex. (C) The wavy upper parts of the low-speed streaks ($y^+ > 10$) are thought to produce wavy sand streaks.

1967; Gupta, Laufer & Kaplan, 1971; Clark & Markland, 1971; Kim, Kline & Reynolds, 1971; Nakagawa & Nezu, 1977, 1981; Praturi & Brodkey, 1978; Sumer & Deigaard, 1981; Smith & Metzler, 1983). The distribution of $\bar{\lambda}_z^+$ is broad and skewed towards higher values, with a standard deviation equal to 30–40% of the mean (Kline *et al.*, 1967; Lee, Eckelman & Hanratty, 1974; Smith & Metzler, 1983). The dimensionless height of the low-speed streaks is:

$$\bar{\lambda}_y^+ \equiv \frac{\bar{\lambda}_y U_*}{\nu} \simeq 30 \qquad (2)$$

where $\bar{\lambda}_y$ is the mean height of the top of the low-speed fluid (Kline *et al.*, 1967; Bakewell & Lumley, 1967; Blackwelder & Eckelmann, 1979). Their dimensionless length is (Cantwell, 1982):

$$\bar{\lambda}_x^+ \equiv \frac{\bar{\lambda}_x U_*}{\nu} \simeq 1000 \qquad (3)$$

where $\bar{\lambda}_x$ is the mean length of the low-speed streaks.

Grass (1971) and Allen (1982) thought that sand streaks were localized under low-speed streaks and therefore should show the same spacing. Existing spacing data for sediment streaks of quartz sand, kaolinite and mica flakes, and for parting lineation as preserved in sandstones (Table 1) show that the spacings of sand streaks and parting lineation are similar to the spacings of the low-speed streaks, but a causal connection is uncertain because several questions remain unanswered.

First, most experiments evaluating equations (1–3) have not exceeded $U_* = 1{\cdot}4 \times 10^{-2}$ m s$^{-1}$, a value close to the critical shear velocities needed to entrain fine- to medium-grained sand. Therefore, it is not known if $\bar{\lambda}_z^+$ remains constant at the higher shear velocities that would characterize normal bedload transport of sand.

Second, very little is known about the effect of a rough boundary on the low-speed streaks. The ejection phase of the burst cycle is more intense over a rough boundary than a smooth one (Grass, 1971; Jackson,

**Table 1.** Sediment streak data

| Author | Grain | Mean diameter (μm) | $U_*$ ($\times 10^{-2}$ m s$^{-1}$) | $\bar{\lambda}_z$ ($\times 10^{-2}$ m) | $\lambda_z^+$ | Comments |
|---|---|---|---|---|---|---|
| Allen (1964) | Quartz sandstones | Fine–medium | Unknown | 0·59–1·25 | | Spacings are Allen's estimates from rocks |
| | Quartz sand | 350 | Not measured | 0·6–2·0 | | Spacings are Allen's estimates from sand streaks in a flume |
| Allen (1968) | Quartz sand | Fine | Not measured | 0·5 | | Experiments not described |
| Allen (1969) | Kaolinite | 4 | 1·1 | 0·80 | 88 | $U_*$ values are whole flume averages from $U_* = (gRS)^{1/2}$ |
| | | | 1·5 | 0·56 | 84 | |
| | | | 2·0 | 0·60 | 120 | |
| Grass (1971) | Quartz sand | 100 | 2·13 | 0·38 | 80 | Spacing is estimated for this study from a photograph |
| Karcz (1973) | Quartz sand | | | 2–8 | | Very little data |
| Mantz (1978) | Mica flakes | 23·5 | 1·02 | 0·65 | 66 | $U_*$ values are whole flume averages from $U_* = (gDS)^{1/2}$. Mean mica streak spacings are estimated for this study from whole distributions |
| | | | 1·17 | 0·54 | 63 | |
| | | 41·5 | 1·24 | 0·68 | 84 | |
| | | | 1·45 | 0·54 | 78 | |
| | | 76·0 | 1·16 | 0·68 | 79 | |
| | | | 1·49 | 0·48 | 72 | |

1976; Nakagawa & Nezu, 1977; Sumer & Deigaard, 1981), the area of the bed affected by an ejection is wider, and ejection velocities are greater. Sumer & Deigaard (1981) suggested that as roughness elements increase in size, the sublayer and its structures are progressively disrupted, a process that would result in a wider spacing of the low-speed streaks. Grass (1971) similarly predicted that increased roughness at the boundary would cause the overall scale of the inrush-ejection eddies to increase. Roughness elements with a dimensionless diameter of $d^+ \geqslant 70$, where $d^+ = dU_*/\nu$, are predicted to destroy the sublayer streaks completely (Grass, 1971; Jackson, 1976). Thus, it may be that with either increasing bedload transport rate or grain size, sand streak spacings will widen and ultimately disappear as the near bed fluid structure is progressively destroyed.

Third, we and others have noticed denser lanes of sediment-laden fluid, about four times as wide as sand streaks, at high shear velocities and high grain concentrations on the bed. Karcz (1973) estimated that the spacing of these features, he called bands, ranged from $2{\cdot}0 \times 10^{-2}$ to $8{\cdot}0 \times 10^{-2}$ m. These clearly are more widely spaced than the low-speed streaks. Neither the origin of this feature nor its preservation potential in sandstones is known.

Fourth, sediment streaks become wavy in plan view above a critical $U_*$ depending on grain size and shape (Allen, 1969; Mantz, 1978). This probably reflects some aspect of the fluid structure, but this has not been investigated.

Fifth, Allen (1964) thought that grain orientation, sorting, and imbrication of grains within modern sand streaks (windrows) and within parting lineation from the Devonian Old Red Sandstone are similar enough to conclude that parting lineation is made of preserved sand streaks. However, his spacing measurements are wider than predicted by equation (1), if one assumes a $U_*$ value characteristic of upper plane bed flow. The reasons for this discrepancy are unknown.

The six experiments reported here were designed to fill in some of these gaps in our knowledge. The purpose of experiments I–IV was to describe the spacings of sand streaks from four sand populations of different mean sizes as functions of the shear velocity and water depth. To inhibit the formation of ripples, sediment feed rates were kept well below the capacity of the flow. The purpose of experiments V and VI was to test the effect of grain concentration on the morphologies and spacings of the sand streaks and on the shapes of accompanying fluid velocity profiles.

## METHODOLOGY

### The flume

The experiments were performed in a wooden open-topped flume 15 m long, 0·33 m wide, and 0·22 m deep that had an adjustable slope and variable water discharge. A test section 6·9 m downstream from the water inlet contained plexiglass sides and a glass bottom. Depth was controlled by adjusting a vertically hinged tail gate. Water temperature varied from 17·0 to 17·5°C during the experiments.

### Procedure

Experiments I–IV consisted of sets of runs at flow depths of $5{\cdot}0 \times 10^{-2}$ and $9{\cdot}0 \times 10^{-2}$ to $1{\cdot}0 \times 10^{-1}$ m, resulting in width/depth ratios of 6·7 and ~3·7. Experiments V and VI were all at the greater depths. An isovel map of a transverse section through the test reach was symmetrical, suggesting large-scale secondary flow was negligible.

The sediment consisted of four $\phi$-normal sand populations, labelled A–D, whose composition and graphic mean sizes are given in Tables 2 and 3. Dry sand was added to the flow approximately 6·5 m upstream from the test section by a vibrating sediment feeder with a variable feed rate. In experiments I–IV the sand feed rate was limited to produce a discontinuous layer of rolling and saltating grains that in some sand streaks became, at most, a few grain diameters thick, but otherwise produced bed concentrations of less than 0·07. Much of the bed was clear of grains. In experiments V and VI sand feed rate was varied to produce bedload transport rates from zero to the capacity of the flow. The bed ranged from relatively grain free to almost completely covered. The mean volume concentration, $C$, of solids in the moving bed layer of thickness, $h$, was calculated from the measured bedload transport rate per unit width, $i_b$, by the formula:

$$C = \frac{i_b}{U_b(\sigma - \rho)h} \tag{4}$$

where $U_b$ is the mean grain velocity, $\sigma$ is the density of the grain, and $\rho$ is the density of the fluid. Mean grain velocity was calculated as (Bridge & Dominic, 1984):

$$\frac{U_b}{V_g} = 10{\cdot}2\frac{U_*}{V_g} - 1{\cdot}1 \tag{5}$$

where $V_g$ is the fall velocity of the mean grain size in

each distribution. The thickness of the moving bed layer was calculated as (Bridge & Dominic, 1984):

$$\frac{h}{\bar{d}} = 2{\cdot}53(\Theta - \Theta_c)^{0{\cdot}5} + 0{\cdot}5 \qquad (6)$$

where $\bar{d}$ is the mean grain diameter of each distribution, $\Theta$ is the dimensionless bed shear stress, and $\Theta_c$ is the $\Theta$ value at the threshold of motion. These concentrations should be considered relative values because we do not have any independent measure of their accuracy.

The strategy of each set of runs was to photograph the sand streaks on the bed at incremented values of the shear velocity, from $U_{*cr}$ to a flow intensity so great that the camera could not capture discrete grain images. That limit occurred at about $U_* = 3{\cdot}5 \times 10^{-2}$ m s$^{-1}$. The method of incrementing $U_*$ was to hold depth constant by adjusting the tail gate, while increasing the total discharge.

Time-averaged fluid velocities were measured with a 1/8 inch O.D. pitot tube at six distances, $y$, off the bed, from $1{\cdot}5 \times 10^{-3}$ to $5{\cdot}0 \times 10^{-2}$ m. The shear velocity, $U_*$, was estimated from the slope of the linear regression equation:

$$V_x = 5{\cdot}75\,U_* \log_{10} y - 5{\cdot}75\,U_* \log_{10} k \qquad (7)$$

where $V_x$ is the $x$-directed velocity at distances $y$, off the bed from just above the viscous sublayer to approximately 20% of the depth, and $k$ is a roughness factor. The variance for repeated $U_*$ measurements at a point under constant hydraulic conditions was $1{\cdot}0 \times 10^{-4}$ m s$^{-1}$. In all experiments $U_*$ was calculated from fluid velocity profiles measured in clear water before the addition of sand. As Gust & Southard (1983) have shown, during even modest bedload transport, fluid velocity profiles overestimate the true shear velocity. We consider the clear water $U_*$ to be accurate for all except the highest bedload transport rates within each set because the discharges and depths in the test reach remained constant. At the highest transport rates the true shear velocities may be lower than our measured values by at most 10% due to the drag reduction caused by the moving grains.

Several photographs of sand streaks were made at each flow intensity. A 35-mm single-lens reflex camera was mounted over the test section at about 0·8 m off the bed providing a streamwise field of view of approximately 0·5 m. A tray of plexiglass (0·22 × 0·58 m) was floated past the test section to eliminate reflections from the water surface. In addition, some photographs were taken from below the flume through a glass window (0·28 × 0·48 m) to avoid interference from suspended grains. Sand streak spacings from both views are similar and are combined here.

Prints at a scale of 1:1·6 were made of the best photographs and three evenly spaced traverse lines were drawn perpendicular to the flow direction. Approximately 100 spacings from each photograph were measured along the traverse lines on a computer-linked digitizing table yielding a mean and standard deviation, a histogram of the spacings, and a plot of the spacing width versus distances across the bed. Streaks in the centre 0·25 m of all photographs showed no variation of spacing with location and hence these were considered to have the equilibrium spacings for the shear velocity measured at the channel centre.

Some decisions were necessary on the part of the operator in deciding which sand structures constituted a streak. A sand streak was defined as a cluster of sand grains as narrow as one grain diameter, with a streamwise extent of at least $3 \times 10^{-2}$ m. This length was based on a ratio of low-speed streak spacing to length of about 1:10 (Kline *et al.*, 1967), and was conservative; very few sand streaks were shorter than $5 \times 10^{-2}$ m. In addition, indistinct or fuzzy areas of the bed were ignored.

In a few runs, sand-starved ripples were allowed to form. In those photographs all sand streaks on the ripple backs were measured instead of using the traverse method. Those spacings are labelled 'R' in Table 2.

## PRESENTATION OF DATA AND DISCUSSION

### Description of sand streaks

#### *Straight sand streaks*

Fine- to medium-grained sands (grain populations A, B and C) move in streaks on the bed from their incipient motion to suspension (Tables 2 and 3). The very coarse grains of population D (experiment IV) do not form sand streaks; the implications will be discussed later with experiments V and VI. The sand streaks are predominantly straight, non-intersecting, and parallel to the flow at flow intensities slightly greater than $U_{*cr}$ (Fig. 2A, B). Sand streak paths as seen from below the flume become more complex with increasing flow intensity, and two distinct sand streak patterns emerge on the bed. Straight sand streaks from populations A and B, and less noticeably from C, occasionally merge and diverge as they move downstream in paths subparallel to the flow (Fig. 2C,

**Table 2.** Flow variables and sand streak data for experiments I–IV

| Flow variables | | | | | | | Sand streak measurements | | | |
|---|---|---|---|---|---|---|---|---|---|---|
| $U_*$ ($\times 10^{-2}$ m s$^{-1}$) | $R^2$ | $\bar{V}$ ($\times 10^{-2}$ m s$^{-1}$) | $k$[1] ($\times 10^{-7}$ m) | Re[2] | Fr[3] | Slope | Depth ($\times 10^{-2}$ m) | Mean spacing, $\lambda_z$ ($\times 10^{-3}$ m) | $\sigma$ St. dev. ($\times 10^{-3}$ m) | $\bar{\lambda}_z{}^{+}$[4] |
| Experiment I (A: garnet sand, $\bar{d}=150$ μm) | | | | | | | | | | |
| 1·79 | 0·98 | 5·04 | 5·0 | 47,911 | 0·52 | 0·0025 | 9·5 | 4·27 | 1·34 | 76 |
| 2·36 | 0·98 | 6·02 | 13·0 | 57,231 | 0·62 | 0·0025 | 9·5 | 3·77 | 1·17 | 89 |
| 2·51 | 0·96 | 7·31 | 3·0 | 69,406 | 0·76 | 0·0025 | 9·5 | 4·28 | 1·64 | 107 |
| 1·83 | 0·96 | 5·28 | 4·0 | 50,126 | 0·55 | 0·0025 | 9·5 | 5·14 | 1·69 | 94 |
| 2·60 | 0·98 | 7·44 | 4·0 | 70,715 | 0·77 | 0·0025 | 9·5 | 4·13 | 1·24 | 107 |
| 2·76 | 0·96 | 8·38 | 2·0 | 79,643 | 0·87 | 0·0025 | 9·5 | 4·38 | 1·40 | 121 |
| 4·89 | 0·98 | 12·02 | 20·0 | 99,760 | 1·25 | 0·0034 | 9·5 | 4·18 | 1·22 | 204 |
| | | | | | | | Mean of means: | 4·33 | | 99 |
| Experiment II (B: quartz sand, $\bar{d}=200$ μm) | | | | | | | | | | |
| 1·88 (R) | 0·90 | 3·97 | 71·0 | 37,753 | 0·41 | 0·00130 | 9·5 | 5·94 | 2·47 | 112 |
| 1·86 | 0·88 | 5·73 | 2·0 | 54,444 | 0·59 | 0·00130 | 9·5 | 4·21 | 1·55 | 78 |
| 2·51 | 0·92 | 7·93 | 3·0 | 75,316 | 0·82 | 0·00130 | 9·5 | 3·92 | 1·35 | 99 |
| 3·03 | 0·96 | 6·77 | 56·0 | 62,267 | 0·70 | 0·00130 | 9·5 | 3·59 | 1·21 | 109 |
| 2·16 (R) | 0·98 | 4·92 | 64·0 | 46,740 | 0·51 | 0·00130 | 9·5 | 4·32 | 1·44 | 93 |
| 1·81 | 0·94 | 5·30 | 4·0 | 47,718 | 0·56 | 0·00130 | 9·0 | 4·41 | 1·36 | 80 |
| 3·60 | 0·98 | 8·08 | 49·0 | 76,741 | 0·84 | 0·00130 | 9·5 | 4·13 | 1·65 | 149 |
| 2·04 (R) | 0·98 | 3·82 | 125·0 | 19,115 | 0·55 | 0·00130 | 5·0 | 4·32 | 1·32 | 88 |
| 2·00 | 0·98 | 4·99 | 13·0 | 24,930 | 0·71 | 0·00140 | 5·0 | 4·66 | 1·54 | 93 |
| 1·86 | 0·98 | 5·07 | 6·0 | 25,330 | 0·72 | 0·00240 | 5·0 | 4·03 | 1·40 | 75 |
| 1·77 | 0·98 | 5·36 | 2·0 | 26,790 | 0·76 | 0·00240 | 5·0 | 3·93 | 1·54 | 69 |
| 1·87 | 0·98 | 4·90 | 17·0 | 24,510 | 0·70 | 0·00520 | 5·0 | 4·64 | 1·48 | 87 |
| 1·35 (R) | 0·98 | 3·53 | 11·0 | 17,636 | 0·50 | 0·00520 | 5·0 | 5·08 | 1·31 | 69 |
| 1·85 (R) | 0·90 | 4·94 | 10·0 | 24,720 | 0·71 | 0·00170 | 5·0 | 5·42 | 1·57 | 100 |
| 1·68 | 0·96 | 6·21 | 1·0 | 31,034 | 0·89 | 0·00190 | 5·0 | 4·50 | 1·19 | 76 |
| 1·97 | 0·96 | 4·59 | 24·0 | 43,619 | 0·48 | 0·00080 | 9·5 | 4·70 | 1·37 | 92 |
| 1·76 | 0·96 | 5·22 | 3·0 | 49,631 | 0·54 | 0·00080 | 9·5 | 4·64 | 1·59 | 82 |
| 2·02 | 0·98 | 4·55 | 23·0 | 23,745 | 0·65 | 0·00080 | 5·0 | 6·76 | 1·84 | 136 |
| 1·64 | 0·98 | 4·47 | 3·0 | 22,328 | 0·64 | 0·00080 | 5·0 | 4·70 | 1·49 | 77 |
| 1·85 | 0·98 | 5·97 | 1·0 | 35,802 | 0·78 | 0·00080 | 6·0 | 3·45 | 1·34 | 64 |
| 2·90 | 0·98 | 7·46 | 14·0 | 70,857 | 0·77 | 0·00080 | 9·5 | 4·25 | 1·40 | 123 |
| | | | | | | | Mean of means: | 4·38 | | 93 |
| Experiment III (C: quartz sand, $\bar{d}=290$ μm) | | | | | | | | | | |
| 1·48 | 0·98 | 3·81 | 13·0 | 36,148 | 0·40 | 0·0017 | 9·5 | 7·27 | 0·230 | 107 |
| 2·74 | 0·98 | 5·57 | 115·0 | 52,953 | 0·58 | 0·0017 | 9·5 | 5·85 | 0·169 | 160 |
| 3·04 | 0·98 | 6·75 | 55·0 | 64,155 | 0·70 | 0·0017 | 9·5 | 4·85 | 0·161 | 148 |
| 2·29 | 0·98 | 5·35 | 31·0 | 50,832 | 0·55 | 0·0017 | 9·5 | 5·70 | 0·188 | 130 |
| 2·54 | 0·98 | 4·85 | 162·0 | 46,037 | 0·50 | 0·0017 | 9·5 | 6·04 | 0·186 | 154 |
| 1·92 | 0·98 | 4·70 | 27·0 | 44,688 | 0·49 | 0·0017 | 9·5 | 5·32 | 0·202 | 102 |
| 1·38 | 0·92 | 4·21 | 3·0 | 39,977 | 0·44 | 0·0017 | 9·5 | 6·29 | 0·211 | 87 |
| 1·85 | 0·87 | 4·03 | 63·0 | 38,281 | 0·42 | 0·0017 | 9·5 | 5·59 | 0·186 | 103 |
| 1·66 | 0·88 | 6·09 | 1·0 | 30,453 | 0·87 | 0·0021 | 5·0 | 5·02 | 0·167 | 83 |
| 0·93 | 0·98 | 3·24 | 1·0 | 16,215 | 0·46 | 0·0021 | 5·0 | 6·06 | 0·165 | 56 |
| 1·51 | 0·98 | 4·98 | 1·0 | 24,869 | 0·71 | 0·0021 | 5·0 | 5·04 | 0·149 | 78 |
| 2·81 | 0·98 | 6·27 | 43·0 | 31,335 | 0·90 | 0·0021 | 5·0 | 5·72 | 0·175 | 160 |
| 1·30 | 0·98 | 4·25 | 1·0 | 21,266 | 0·61 | 0·0016 | 5·0 | 6·16 | 0·209 | 80 |
| 2·50 | 0·98 | 4·30 | 155·0 | 21,480 | 0·61 | 0·0016 | 5·0 | 5·84 | 0·189 | 146 |
| 1·98 | 0·98 | 4·98 | 11·0 | 24,920 | 0·71 | 0·0016 | 5·0 | 5·39 | 0·161 | 107 |
| 1·65 | 0·98 | 4·92 | 3·0 | 24,545 | 0·70 | 0·0029 | 5·0 | 5·66 | 0·173 | 93 |
| 2·48 | 0·90 | 6·57 | 16·0 | 60,399 | 0·69 | 0·0029 | 9·2 | 5·37 | 0·177 | 133 |
| 3·33 | 0·98 | 8·59 | 14·0 | 81,586 | 0·89 | 0·0025 | 9·5 | 4·40 | 0·130 | 147 |
| 2·63 | 0·98 | 6·27 | 31·0 | 59,573 | 0·65 | 0·0025 | 9·5 | 4·64 | 0·148 | 122 |
| | | | | | | | Mean of means: | 5·59 | | 116 |
| Experiment IV (D: quartz sand, $\bar{d}=1380$ μm). No sand streaks observed | | | | | | | | | | |

[1] Roughness constant from equation (7); [2] Reynold's number; [3] Froude number; [4] Dimensionless sand streak spacing; R indicates isolated ripples present.

**Table 3.** Flow variables and sand streak data for experiments V and VI

| | | Flow variables | | | | | | | Sand streak measurements | | | |
|---|---|---|---|---|---|---|---|---|---|---|---|---|
| | Mean volume concentration, $C$ | $U_*$ ($\times 10^{-2}$ m s$^{-1}$) | $R^2$ | $\bar{V}$ ($\times 10^{-1}$ m s$^{-1}$) | $k^1$ ($\times 10^{-7}$ m) | Re$^2$ | Fr$^3$ | Slope | Depth ($\times 10^{-2}$ m) | Mean spacing, $\lambda_z$ ($\times 10^{-3}$ m) | $\sigma$ St. dev., ($\times 10^{-3}$ m) | $\lambda_z{}^{*4}$ |
| Experiment V (B: quartz sand, $\bar{d}=200\,\mu$m) | | | | | | | | | | | | |
| Set 1 | 0·013 | 2·04 | 0·94 | 4·64 | 50·0 | 43,781 | 0·48 | 0·00041 | 9·5 | 4·79 | 1·46 | 103 |
| | 0·019 | | | | | | | | | 4·73 | 1·37 | 102 |
| | 0·044 | | | | | | | | | 4·41 | 1·35 | 95 |
| | 0·089 | | | | | | | | | 4·60 | 1·31 | 99 |
| Set 2 | 0·000 | 3·19 | 0·99 | 7·71 | 22·0 | 73,217 | 0·80 | 0·00041 | 9·5 | — | — | — |
| | 0·005 | | | | | | | | | 4·10 | 1·09 | 131 |
| | 0·009 | | | | | | | | | 4·31 | 1·31 | 137 |
| | 0·012 | | | | | | | | | 4·47 | 1·30 | 143 |
| | 0·024 | | | | | | | | | 4·27 | 1·50 | 136 |
| | 0·075 | | | | | | | | | 4·25 | 1·34 | 136 |
| | 0·169 | | | | | | | | | 4·60 | 1·33 | 147 |
| | 0·362 | | | | | | | | | 5·20 | 1·95 | 166 |
| Set 3 | 0·000 | 1·51 | 0·99 | 3·65 | 24·0 | 34,675 | 0·38 | 0·00041 | 9·5 | — | — | — |
| | <0·001 | | | | | | | | | 5·59 | 2·04 | 84 |
| | 0·006 | | | | | | | | | 5·90 | 1·86 | 89 |
| | 0·023 | | | | | | | | | 5·38 | 1·80 | 81 |
| | 0·027 | | | | | | | | | 5·41 | 1·54 | 82 |
| | 0·055 | | | | | | | | | 5·58 | 2·02 | 84 |
| | 0·154 | | | | | | | | | 6·14 | 1·93 | 83 |
| Experiment VI (C: quartz sand, $\bar{d}=290\,\mu$m) | | | | | | | | | | | | |
| Set 1 | 0·000 | 2·19 | 0·92 | 7·44 | 1·0 | 67,491 | 0·79 | 0·0029 | 9·0 | — | — | — |
| | 0·025 | | | | | | | | | 5·68 | 1·14 | 124 |
| | 0·039 | | | | | | | | | 5·79 | 1·53 | 126 |
| | 0·067 | | | | | | | | | 5·65 | 1·51 | 124 |
| | 0·170 | | | | | | | | | 6·59 | 2·03 | 144 |
| Set 2 | 0·000 | 2·60 | 0·97 | 6·44 | 18·0 | 64,440 | 0·65 | 0·0014 | 10·0 | — | — | — |
| | 0·016 | | | | | | | | | 5·51 | 1·81 | 143 |
| | 0·031 | | | | | | | | | 5·48 | 1·44 | 143 |
| | 0·045 | | | | | | | | | 5·64 | 1·38 | 147 |
| | 0·094 | | | | | | | | | 6·44 | 1·98 | 167 |
| Set 3 | 0·000 | 2·45 | 0·99 | 7·43 | 2·0 | 77,966 | 0·73 | 0·0014 | 10·5 | — | — | — |
| | 0·041 | | | | | | | | | 5·71 | 1·94 | 140 |
| | 0·077 | | | | | | | | | 5·81 | 1·90 | 142 |
| | 0·153 | | | | | | | | | 6·12 | 1·88 | 150 |
| | 0·390 | | | | | | | | | 6·67 | 1·71 | 163 |

[1] Roughness constant from equation (7); [2] Reynold's number; [3] Froude number; [4] Dimensionless sand streak spacing.

D). Occurring on the bed at the same time as the subparallel sand streaks but of smaller size are zones of *en échelon* sand streaks oblique to the flow direction (Fig. 2E, F). These two patterns emerge from straight flow-parallel sand streaks, quickly disappear, and reappear on another part of the bed. The duration of time sand streaks move in these two patterns appears to be a function of flow intensity. They are obvious features in all photographs for runs with $U_*$ greater than $3\times10^{-2}$ m s$^{-1}$, appear in some of the photographs for runs with $U_*$ between 2 and $3\times10^{-2}$ m s$^{-1}$, and are rare in the runs at lower flow intensities. It was also noted that the sand streaks persist in any one location for periods much longer than the accepted bursting period.

*Discussion*

These patterns are best explained by grain paths associated with the lifting phase of the burst cycle. The periodic decay of a low-speed streak proceeds in three steps: a gradual lifting away from the wall, more energetic oscillation, and chaotic ejection into the outer flow (Clark & Markland, 1971; Kim *et al.*, 1971). The most common oscillation mode is the development of a single streamwise vortex growing out of the low-speed streak. The straight, non-intersecting, flow-

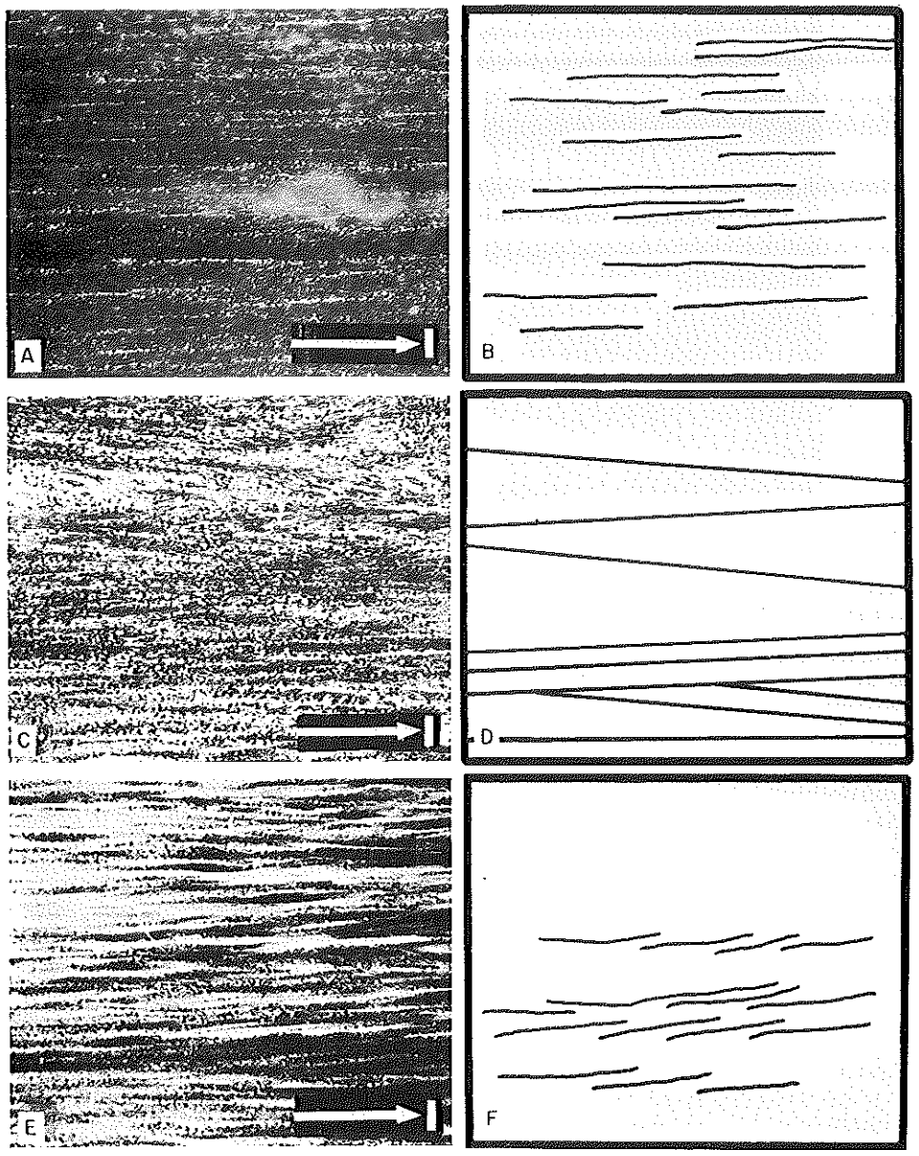


**Fig. 2.** Morphology of quartz sand streaks on a glass plate under sand-starved conditions and water depth equal to $9{\cdot}5 \times 10^{-2}$ m. Scale is $1 \times 10^{-2}$ m and arrows point downstream. View from below bed (A) and interpretation (B) for fine sand with $U_* = 1{\cdot}64 \times 10^{-2}$ m s$^{-1}$ shows straight, flow-parallel, non-intersecting streaks thought to form directly under the low-speed streaks. View from below bed (C) and interpretation (D) for medium sand with $U_* = 2{\cdot}37 \times 10^{-2}$ m s$^{-1}$ shows straight but flow-oblique, intersecting streaks thought to form under the oscillating low-speed streaks. View from above the bed (E) and interpretation (F) for fine sand with $U_* = 2{\cdot}0 \times 10^{-2}$ m s$^{-1}$ shows *en échelon* streaks thought to form under streamwise vortices (see Fig. 1).

parallel sand streaks mostly likely are formed under relatively stable but slowly lifting low-speed streaks as suggested by Allen (1982). The merging and diverging sand streaks and the *en échelon* sand streaks are thought to reflect the fluid paths in this streamwise vortex. These two patterns are observed more frequently at higher flow intensities because the burst rate is a function of shear velocity.

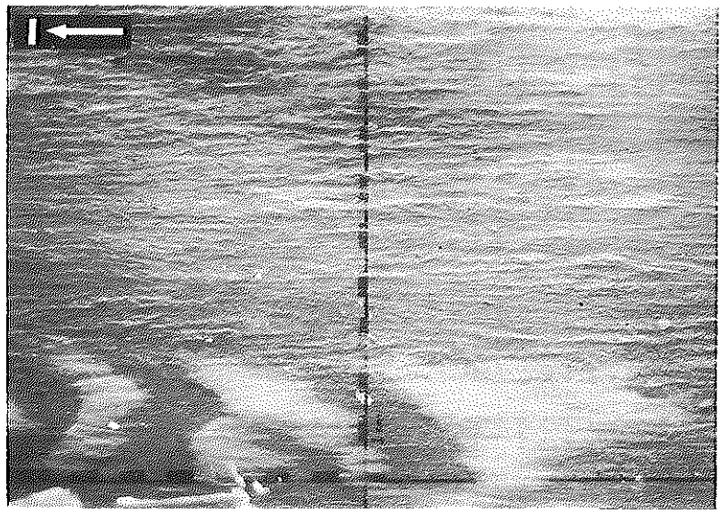

**Fig. 3.** Wavy sand streaks of fine quartz sand as seen from above the bed. Scale is $1 \times 10^{-2}$ m and arrow points downstream. $U_* = 1{\cdot}81 \times 10^{-2}$ m s$^{-1}$, $d = 200$ μm, and flow depth $= 9{\cdot}5 \times 10^{-2}$ m. Waviness results from sand grains at least partly suspended in the upper wavy portion of a low-speed streak (Fig. 1C).

The persistence of sand streaks is a reflection of the persistence of low-speed streaks whose durations as identifiable units on the bed may be as long as $t^+ \simeq 2000$ (Smith & Metzler, 1983).

*Wavy sand streaks*

At flow intensities greater than $U_* \cong 1{\cdot}8 \times 10^{-2}$ m s$^{-1}$ for fine sand and $2{\cdot}2 \times 10^{-2}$ m s$^{-1}$ for medium sand, streaks viewed from above the bed are distinctly wavy, as shown in Fig. 3. In addition, all sand streaks on ripples are wavy when viewed from above. Mantz (1978) noted the change from straight sediment streaks to wavy ones with increasing flow intensity in mica flakes.

*Discussion*

The waviness probably reflects the motion of grains suspended in the lifting low-speed streak (Fig. 1). Kline *et al.* (1967) showed that hydrogen bubble paths were distinctly wavy for $y^+$ between 9·6 and 38 or, with $U_* = 1{\cdot}8 \times 10^{-2}$ m s$^{-1}$ in water, for $y$ between $5{\cdot}3 \times 10^{-4}$ and $2{\cdot}1 \times 10^{-3}$ m. An approximate criterion for a grain to be suspended in this zone is (Francis, 1973):

$$\frac{V_g}{U_*} \leqslant 1 \qquad (8)$$

where $V_g$ is the grain fall velocity. Thus there should be a correlation between the shear velocity at the onset of waviness and grain size, if grain density is held constant. A plot of $U_*$ at the onset of waviness versus mean grain size for grains from this study and from Mantz (1978) (Fig. 4) shows a good correlation

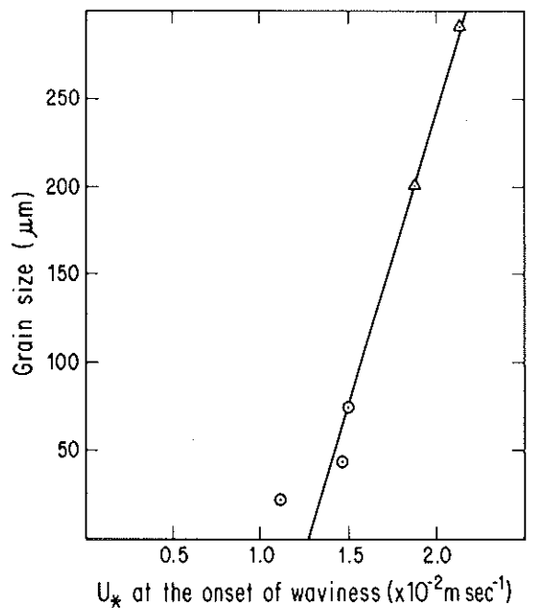


**Fig. 4.** $U_*$ at the onset of waviness in streaks of sand (○) and mica flakes (△) versus grain size. The linear regression equation is: $d_{mm} = 0{\cdot}28$, $U_* - 0{\cdot}33$ with $R^2 = 0{\cdot}94$. The relationship is thought to indicate that waviness of sand streaks results from grains travelling above $y^+ \simeq 9{\cdot}6$, in the zone of wavy low-speed streaks. Mica data are from Mantz (1978).

even though the $U_*$ values are calculated by different methods, the onset of waviness is estimated, and the grain shapes are quite variable. (Grain size was chosen over fall velocity because the fall velocity for Mantz's mica flakes is unavailable and impossible to predict.)

*Absence of sand streaks*

Under sand-starved conditions fine-grained sand forms well-defined sand streaks, medium-grained sand forms less well-defined streaks, and very coarse sand (population D) forms no streaks at all. Allen (1970) suggested that a limit to streak spacing should occur with increasing flow intensity as sand streak spacing approaches the mean grain diameter. In experiments III and IV the mean grain diameters fall between 290 and 1380 μm whereas an average sand streak spacing from experiments I, II and III is approximately 5000 μm. Therefore, for the flow intensities studied, the observed low-speed streak spacings are from 4 to 17 times the diameter of the largest grains. Clearly, the coarsest sand is small enough to be contained within the low-speed streak structure. The mechanisms responsible for the apparent disruption of the streaks by grain size will be discussed under experiments V and VI.

## Sand streak spacings

*Low grain concentrations*

Flume and spacing data for fine- and medium-grained sand (experiments I–III) are listed in Tables 2 and 3. Run 7 ($U_* = 4{\cdot}89 \times 10^{-2}$ m s$^{-1}$) of experiment I is not included here because the sediment feed rate necessary to obtain photographs of sand streaks was much greater than for the other 46 runs.

Histograms of sand streak spacings measured in any one run from experiments I–III are skewed toward higher values (Fig. 5) and have, across all grain sizes, a standard deviation of $\bar{\lambda}_z{}^+$ of about 25% of the grand mean. These are similar to the distributions of low-speed streaks (Lee *et al.*, 1974).

The grand mean of the dimensionless sand streak spacings for fine garnet sand (Table 2) is slightly smaller than the grand mean for the fine quartz sand although not statistically significantly so at these sample sizes. More importantly, the grand mean of both are statistically equivalent to the mean dimensionless spacing of the low-speed streaks given by equation (1). In contrast, the grand mean spacing of the medium-grained quartz sand is statistically significantly larger than the grand means of either the fine sands or the low-speed streaks.

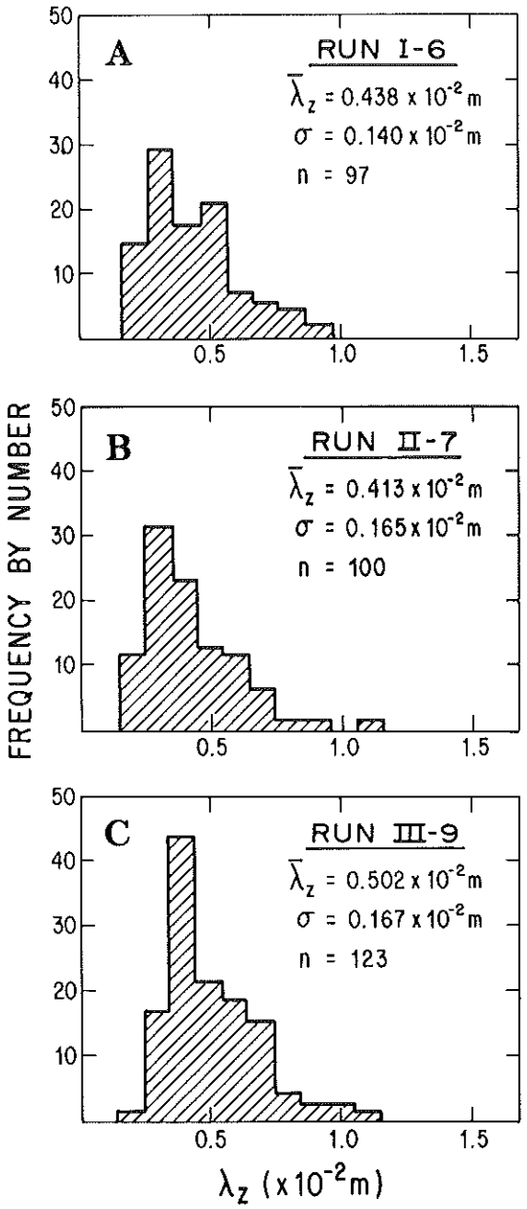


**Fig. 5.** Histograms of sand streak spacings from representative runs. (A) fine garnet sand, $\bar{d} = 150$ μm; (B) fine quartz sand, $\bar{d} = 200$ μm; (C) medium quartz sand, $\bar{d} = 290$ μm. The distributions are broad and skewed towards higher spacings similar to low-speed streak distributions. The medium sand has a significantly larger spacing than the fine sand or low-speed streaks.

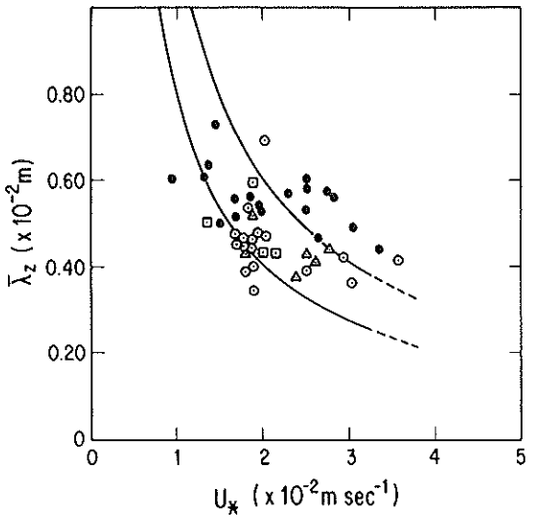


**Fig. 6.** Sand streak spacings, $\bar{\lambda}_z$, versus shear velocity, $U_*$, for grain population A (fine garnet sand, △); grain population B (fine quartz sand, ○), and grain population C (medium quartz sand, ●). Sand streak spacings measured on ripples composed of population B are denoted by (□) and are not significantly different from those on a flat bed. Curves are $\bar{\lambda}_z^+ = 80$ and 120, the span of accepted values of measured spacings for low-speed streaks. Populations A and B produce sand streak spacings similar to low-speed streaks whereas population C produces wider spacings than low-speed streaks.

Figure 6 shows the mean sand streak spacing for each run plotted versus shear velocity. It is obvious that the wider spacing for medium sand is not caused by extreme values; most streaks of medium sand plot above those of fine sand for the same $U_*$ and a cluster ($U_* > 2{\cdot}5 \times 10^{-2}$ m s$^{-1}$) fall above the upper confidence interval of the scaling function for low-speed streaks. In fact, $\bar{\lambda}_z$ is not statistically correlated with $U_*$ for any of the grain sizes. Equation (1) is not a very precise measure of sand streak spacing because of the variability of $\bar{\lambda}_z$ at any one $U_*$. Also shown are the spacings of sand streaks on ripple backs. These are not statistically different from the spacings on the flume bottom.

*High grain concentrations*

Experiments I–IV were designed to allow comparison of sand streak data with fluid streak data and by necessity used sand-starved conditions. The results can be criticized here because possibly not enough sand was available on the bed to form streaks at the smallest wavelengths, and because differing grain concentrations on the bed may have caused some of the spread in the data. Also, the influence of a moving bedlayer on the near-bed, burst structures remains unexamined, prohibiting an extrapolation to current lineation spacing. Experiments V and VI in which the sediment feed rate was a controlled variable were designed to determine the influence of grain concentration on sand streak spacing and near-bed fluid velocity profiles. Table 3 and Figs 7–9 present the data.

Comparing Figs 6 and 7 shows that the spacings of sand streaks with higher grain concentrations on the bed are similar to the spacings of the sand-starved streaks. Coarse sand again yields a wider spacing than fine at a given shear velocity and for the fine sand, equation (1) is an adequate, albeit poor, predictor of $\bar{\lambda}_z$.

The influence of sediment concentration on sand streak spacing is important however, at concentrations above $C \sim 0{\cdot}1$ and especially for the medium sand (Table 3 and Fig. 7). In five of the six sets of data, the highest sediment concentrations on the bed produce

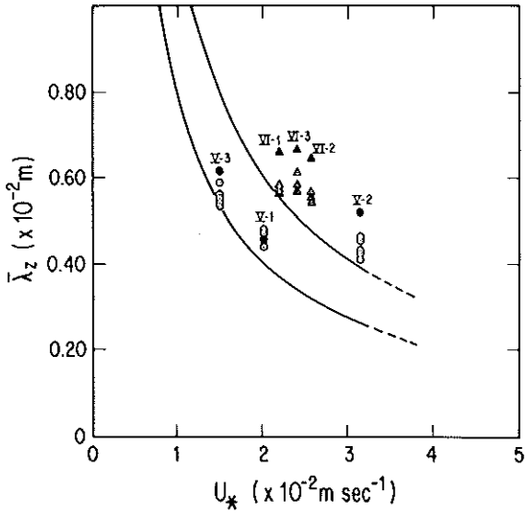


**Fig. 7.** Sand streaks spacings, $\bar{\lambda}_z$, versus shear velocity, $U_*$, for grain populations B (○) and C (△). Each experiment consisted of three sets of runs at varying shear velocities, and each set consisted of numerous runs of varying grain concentrations on the bed, the highest of which is marked by a solid symbol. At low grain concentrations the spacings fall in the same domain as in the sand-starved case (see Fig. 6). At the highest grain concentrations, the spacings are wider and fall farther outside the band for the low-speed streaks denoted by the curves.

the widest sand streak spacings. Below 0·1 in the range of concentrations used in experiments I–IV, and especially for the fine sand, spacing seems independent of grain concentration, the variation in spacing at any $U_*$ being attributable to the variation in $\bar{\lambda}_x{}^+$ of low-speed streaks plus experimental error.

High sediment concentrations also modify the vertical profiles of fluid velocity causing a retardation of flow near the bed (Fig. 8). This increases the shear velocity calculated from a log $y$ versus $V$ plot. Because the flow Reynolds number did not change appreciably with increasing sediment concentration on the bed we conclude, as did Gust & Southard (1983), that the true shear velocity remained unchanged from the clear water value and the deviation from the law of the wall reflects a change in the flow structure near the top of the moving bed layer.

It is also of considerable interest that, at shear velocities greater than $2{\cdot}5 \times 10^{-2}$ m s$^{-1}$, and at higher grain concentrations, a secondary spacing of sand streaks appears ($\lambda \simeq 1{\cdot}5 \times 10^{-2}$ m) manifested by denser, often arcuate lanes of sand (Fig. 9). The cleared parts of the bed and the associated skewed radial pattern formed by grains are assumed to be the imprint of the massive inflow of the burst cycle on the bed. It appears that this inflow sweeps grains to the side, increasing their concentration in the sand streaks there and causing the secondary spacing.

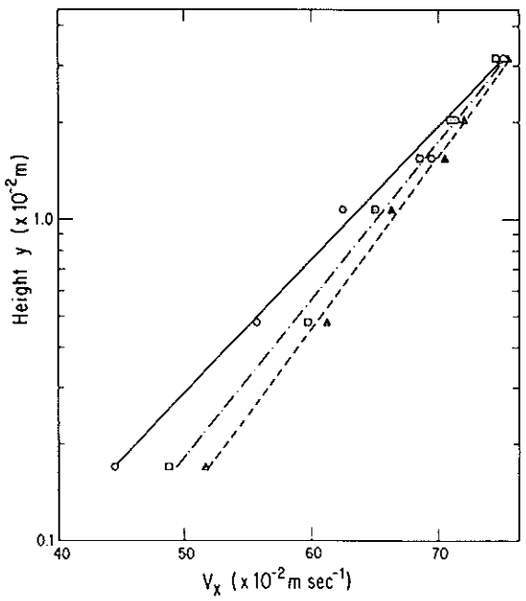


**Fig. 8.** Logarithmic velocity profiles for runs 1, 7 and 8, set 2, experiment V, showing a retardation of fluid velocity below about $3 \times 10^{-2}$ m with increasing mean volume concentration of medium quartz sand in the moving bed layer. Clear water (△); C=to 0·17 (□); C=to 0·36 (○). The apparent shear velocities increase from 3·2 to 3·4 to $4{\cdot}3 \times 10^{-2}$ m s$^{-1}$ with increasing grain concentration even though the true shear velocity remained at $3{\cdot}2 \times 10^{-2}$ m s$^{-1}$.

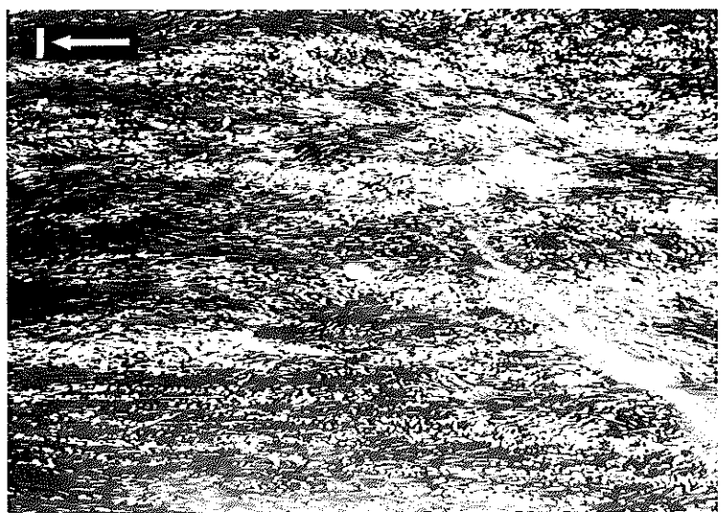

**Fig. 9.** A time lapse view of medium-grained sand streaks from below the flume showing the effect of the inrush phase (sweep) of the burst cycle on sand grains, and the resulting secondary streak spacing. The lanes and associated skewed radial pattern upstream are the imprint of the sweep. The shear velocity $= 2{\cdot}0 \times 10^{-2}$ m s$^{-1}$ and the depth $= 9{\cdot}5 \times 10^{-2}$ m.

## ADDITIONAL COMMENTS AND CONCLUSIONS

The observations described in the previous sections indicate that the present explanation for the origin of sand streaks and parting lineation is not adequate. Medium- and coarse-grained sands, or grain concentrations on the bed typical of moderate and greater bedload transport over a loose sand bed, produce sand streak spacings wider than predicted by the low-speed streak model. Superimposed on these streaks at higher shear velocities and grain concentrations on the bed is a much wider ($\bar{\lambda}_z \simeq 1{\cdot}5 \times 10^{-2}$ m), secondary spacing of sand streaks. And very coarse sand, comprising a transitionally rough bed, does not form streaks even though the grains are still many diameters smaller than the predicted spacing.

In addition, the following observations are considered important:

(1) the low-speed streak model *is* an adequate predictor of sand streak spacings and morphologies at low sediment concentrations on the bed and for grain sizes less than medium-grained sand;

(2) sand streaks become wavy in plan view at a threshold shear velocity that seems to correlate with grain size;

(3) fluid velocities are retarded in the zone immediately above the moving bed layer for bedload concentrations greater than approximately 0·15 for fine sand and 0·02 for medium sand.

At the present time we can only speculate on a possible explanation for these observations. Gust & Southard (1983) noted, as we did, a retardation of streamwise fluid velocities up to $y^+ \simeq 600$ above a carpet of *rolling* grains. They hypothesized that a new kind of fluid flow may be created directly above the moving bed layer for which the mechanics of fluid momentum transfer are different from those over a fixed bed. The manifestations of this new type of flow are a replacement of the viscous sublayer with an extension of the overlying logarithmic layer, a reduction in the von Karman constant, a reduction in the frictional drag, and an increase in the roughness length. Other workers (Yalin, 1977; Adams & Weatherly, 1981) have shown that suspended sediment also substantially reduces turbulent kinetic energy, the von Karman constant, and frictional drag. Adding polymers to water reduces the rate of turbulent energy dissipation, and hence the frictional drag and von Karman constant, by inhibiting the formation of low-speed streaks (Donohue, Tiederman & Reischman, 1972). Even for dilute polymer solutions, $\bar{\lambda}_z^+$ is increased by up to a factor of 1·75. The reductions in frictional drag and the von Karman constant seen in flows over rolling grains, in flows containing suspended solids, and in flows containing polymers suggest a common cause—a decrease in the number of low-speed streaks formed per unit time. Using the percentage drag reduction as a measure of similarity between flows with polymers and flows with rolling grains yields an expected streak spacing over rolling grains of from $\frac{1}{3}$ to $\frac{2}{3}$ again as wide, commensurate with our data.

It is not clear what causes the decrease in the number of low-speed streaks formed per unit time. Donohue *et al.* (1972) suggested that in dilute polymer flows the macromolecules inhibit stretching of the spanwise vortex elements. Possibly suspended sediment has the same effect. Grass (1971) thought that as boundary roughness increases the overall scale of the inrush and ejection eddies would also increase. This would decrease the number and regularity of low-speed streaks. An increase in either grain size, grain concentration, or thickness of the moving bedlayer would increase boundary roughness.

In either case, the evolution of low-speed streaks and sand streaks with increasing sediment concentration in the moving bedlayer may be the following. At relatively low sediment concentration and for finer than medium sand, the bed is hydraulically smooth, a viscous sublayer exists, and low-speed streaks are well developed. Straight sand streaks are formed with $\bar{\lambda}_z^+ \simeq 100 \pm 20$. At higher shear velocities fine-grained sand experiences partly suspended saltation, rising to heights of $y^+ \simeq 10$ and the sand streaks become wavy in plan view. Simultaneously, the increasing grain concentration or grain size of the moving bedlayer destroys the viscous sublayer, reduces overlying fluid velocities and increases the spacing and irregularity of the low-speed streaks. The wider spacing of sand streaks and parting lineation may reflect this.

## ACKNOWLEDGMENTS

This research was conducted by S. Weedman as partial fulfillment of the requirements for the Masters Degree and was funded by NSF Grant No. EAR-8117050 awarded to R. Slingerland. Thanks go to John Bridge and referees for weighty comments on the manuscript and to Steven Read, Kathleen Gerety, Henry Hanson, Arthur Miller, Judy Bailey and Larry Robinson for help and encouragement.

## REFERENCES


ADAMS, C.E. & WEATHERLY, G.L. (1981) Suspended sediment transport and benthic boundary-layer dynamics. In: *Sedimentary Dynamics of Continental Shelves* (Ed. by C. A. Nittrower). *Developments in Sedimentology*, **32**, 449 pp.

ALLEN, J.R.L. (1964) Primary current lineation in the Lower Old Red Sandstone, (Devonian), Anglo-Welsh Basin. *Sedimentology*, **3**, 89–108.

ALLEN, J.R.L. (1968) The nature and origin of bed-form hierarchies. *Sedimentology*, **10**, 161–182.

ALLEN, J.R.L. (1969) Erosional current marks of weakly cohesive mud beds. *J. sedim. Petrol.* **39**, 607–623.

ALLEN, J.R.L. (1970) *Physical Processes in Sedimentation*, pp. 67–70. Allen & Unwin, London.

ALLEN, J.R. (1982) *Sedimentary Structures*, pp. 237–270. *Developments in Sedimentology*, **30A**. Elsevier, Amsterdam.

ALLEN, J.R.L. & LEEDER, M.R. (1980) Criteria for the instability of upper-stage plane beds. *Sedimentology*, **27**, 209–217.

BAKEWELL, H.P. & LUMLEY, J.L. (1967) Viscous sublayer and adjacent wall region in turbulent pipe flow. *Phys. Fluids*, **10**, 1880–1889.

BLACKWELDER, R.F. & ECKELMANN, H. (1979) Streamwise vortices associated with the bursting phenomenon. *J. Fluid Mech.* **94**, 577–594.

BRIDGE, J.S. & DOMINIC, D.F. (1984) Bed-load grain velocities and sediment transport rates. *Wat. Resour. Res.* (in press).

CANTWELL, B.J. (1982) Organized motion in turbulent flow. *Ann. Rev. Fluid Mech. 1981*, **13**, 457–515.

CLARK, J.A. & MARKLAND, E. (1971) Flow visualization in turbulent boundary layers. *J. hydraul. Div. Am. Soc. civ. Engrs* **97**, 1653–1664.

DONOHUE, G.L., TIEDERMAN, W.G. & REISCHMAN, M.M. (1972) Flow visualization of the near-wall region in a drag-reducing channel flow. *J. Fluid. Mech.* **56**, 559–575.

FRANCIS, J.R.D. (1973) Experiments on the motion of solitary grains along the bed of a turbulent stream. *Proc. R. Soc. A*, **332**, 443–471.

GRASS, A.J. (1971) Structural features of turbulent flow over smooth and rough boundaries. *J. Fluid Mech.* **50**, 233–255.

GUPTA, A.K., LAUFER, J. & KAPLAN, R.E. (1971) Spatial structure in the viscous sublayer. *J. Fluid Mech.* **50**, 493–512.

GUST, G. & SOUTHARD, J.B. (1983) Effects of weak bed load on the universal law of the wall. *J. geophys. Res.* **88**, C10, 5939–5952.

JACKSON, R.G. (1976) Sedimentological and fluid-dynamic implications of the turbulent bursting phenomenon in geophysical flows. *J. Fluid Mech.* **77**, 531–560.

KARCZ, I. (1970) Possible significance of transition flow patterns in interpretation of origin of some natural bed forms. *J. geophys. Res.* **75**, no. 15, 2869–2873.

KARCZ, I. (1973) Reflection on the origin of some small-scale longitudinal streambed scours. In: *Fluvial Geomorphology* (Ed. by M. Morisawa), pp. 149–173. SUNY, Binghampton.

KIM, H.T., KLINE, S.J. & REYNOLDS, W.C. (1971) The production of turbulence near a smooth wall in a turbulent boundary layer. *J. Fluid Mech.* **50**, 133–160.

KLINE, S.J., REYNOLDS, W.C., SCHRAUB, F.A. & RUNDSTADLER, P.W. (1967) The structure of turbulent boundary layers. *J. Fluid Mech.* **30**, 741–773.

LEE, M.K., ECKELMAN, L.D. & HANRATTY, T.J. (1974) Identification of turbulent wall eddies through phase relation of the components of the fluctuating velocity gradient. *J. Fluid Mech.* **66**, 17–33.

LEEDER, M.R. (1981) *Sedimentology*, pp. 47–66. Allen & Unwin, London.

MANTZ, P.A. (1978) Bedforms produced by fine cohesionless, granular and flakey sediments under subcritical water flows. *Sedimentology*, **25**, 83–103.

NAKAGAWA, H. & NEZU, I. (1977) Prediction of the contributions to the Reynolds stress from bursting events in open channel flows. *J. Fluid Mech.* **80**, 99–128.

NAKAGAWA, H. & NEZU, I. (1981) Structure of space-time correlations of bursting phenomena in an open-channel flow. *J. Fluid Mech.* **104**, 1–43.

PRATURI, A.K. & BRODKEY, R.S. (1978) A stereoscopic visual study of coherent structures in turbulent shear flow. *J. Fluid Mech.* **89**, 251–272.

SMITH, C.R. & METZLER, S.P. (1983) The characteristics of low-speed streaks in the near-wall region of a turbulent boundary layer. *J. Fluid Mech.* **129**, 27–54.

SORBY, H.C. (1908) On the application of quantitative methods to the study of the structure and history of rocks. *Q. Jl geol. Soc. Lond.* **64**, 171–232.

STOKES, W.L. (1953) Primary sedimentary trend indicators as applied to ore finding in the Carrizo Mountains, Arizona and New Mexico. *Rep. Congr. atom. Energy Commn U.S.* RME 3043 (1), 23.

SUMER, B.M. & DEIGAARD, R. (1981) Particle motions near the bottom in turbulent flow in an open channel. Part 2. *J. Fluid Mech.* **109**, 311–337.

YALIN, M.S. (1977) *Mechanics of Sediment Transport*. Pergamon Press, Oxford. 298 pp.


(*Manuscript received 2 November 1983; revision received 14 March 1984*)